

# **MICROSTRIP VEHICULAR ANTENNA FOR MOBILE-SATELLITE COMMUNICATIONS**

H.M.S.B. Senavirathna and I.J.Dayawansa  
Department of Electronic and Telecommunication Engineering  
University of Moratuwa

## MICROSTRIP VEHICULAR ANTENNA FOR MOBILE-SATELLITE COMMUNICATIONS

H.M.S.B. Senavirathna and I.J. Dayawansa

*Department of Electronic and Telecommunication Engineering  
University of Moratuwa*

### ABSTRACT

Circularly polarized antennas are used in mobile-satellite or MSAT communication systems. This reduces the polarization mismatch due to the rotational orientation between the transmitter and the receiver and it also minimizes the interference from multipath reflections. Circularly polarized microstrip antennas are commonly used in these systems because of compactness, the light-weight and the low-profile. It eases the installation on a vehicular body or on the surface of a satellite.

This paper presents a circularly polarized microstrip circular patch antenna designed for vehicular use for MSAT communications at a frequency of around 1.6GHz. It has right-hand circular polarization (RHCP) and near hemispherical coverage needed by the user. The antenna was first simulated using MatLab software for  $TM_{110}$  resonance mode and fabricated on a substrate of epoxy glass fiber. The antenna was tested on a curved ground plane, which was similar to the surface of a vehicle. This low profile microstrip antenna is suitable for vehicle rooftop mounting.

A combination of the resonance cavity model and the transmission-line model was used to analyze the antenna, which consists of a single circular patch as the driven element. In order to obtain circular polarization, perturbation segments to the perimeter of the patch were inserted with a single probe feed on the  $45^\circ$  axis with respect to the perturbation segments, known as mode-de-tuning. As such no external phasing network is required to obtain the  $90^\circ$  time phase difference required for circular polarization. It was fed with a  $50\Omega$  coaxial feed line which was soldered to the inset probe. By adjusting the area of the perturbation segments circular polarization and a good axial ratio was obtained. Half power beam widths of the antenna are  $115^\circ$  in the H plane and  $105^\circ$  in the E plane. The antenna has a gain of 5.7dBi and a bandwidth of 286MHz which is approximately 17% of the centre frequency. The design criteria and performance of the circularly polarized microstrip antenna, which is suitable for MSAT communications, are presented.

### INTRODUCTION

A mobile satellite communication system or a MSAT system requires a circularly polarized ground base antenna having a broad radiation pattern that will provide near hemispherical coverage in the vertical and horizontal planes. Hemispherical coverage is vital for the vehicular antenna so that the mobile can communicate with the satellite from any elevation as shown in Fig.1.

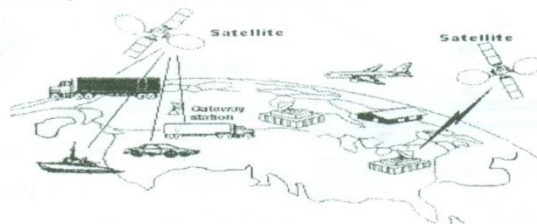


Fig. 1. MSAT Environment

If the transmitted signal is linearly polarized and the receiver antenna is also linearly polarized, then the receiver may not receive the signal satisfactorily due to polarization mismatch[1]. This is a consequence of the faraday rotation caused by the ionosphere which rotates a linearly polarized signal out of alignment. Therefore circular polarization is essential at frequencies of operation below 3GHz where the faraday rotation would cause this problem of polarization mismatch, if the transmitted signal is linearly polarized.

Normally, the signal transmitted in a MSAT communication system would be right hand circularly polarized. The receiving antenna fixed on a vehicle would be a whip antenna or something similar. They are relatively bulky and complex having a broad radiation pattern. This paper suggests a more appropriate antenna for vehicles for MSAT reception. It is a microstrip antenna or a patch antenna, which is a light-weight low-profile antenna. It can receive circularly polarized signals at a frequency near 1.6GHz. It has a very broad radiation pattern in both the E-plane and the H-plane. It can be easily made and can be easily mounted on the roof of a vehicle as shown in Fig:2.

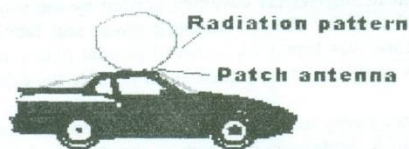


Fig. 2. Mobile installation

During the last two decades patch antennas have gained acceptance for microwave and millimeter wave applications for its simplicity in addition to the other advantages such as compactness, low-profile low-weight, easy to make and easy to integrate nature. This paper describes a circular patch antenna that was designed and tested for the first time in Sri Lanka. It is a RHCP antenna, which operates satisfactorily in the frequency range 1.12 GHz and 1.68GHz.

### CIRCULAR PATCH ANTENNA

A circular patch antenna consists of a small circular metal patch defined on a thin dielectric substrate. On the other side of the substrate is a metal layer which acts as the ground plane as shown in Fig:3.

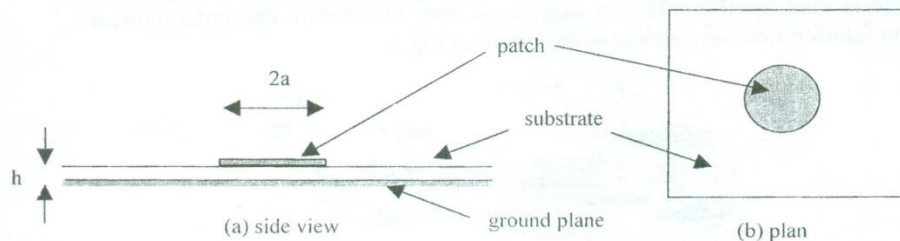


Fig:3 Circular Patch Antenna

When a signal is applied across the patch and the ground plane, the patch radiates in the broadside direction. The patch behaves as a leaky resonator and the leakage constitutes the radiation. In the receive mode, the incident waves excite the patch into resonance and a voltage is developed across the patch and the ground plane. A patch was designed to resonate in the  $TM_{110}$  mode and the  $50\Omega$  matched position was selected for feeding with a  $50\Omega$  line.

### Radiated Field

For the patch behaving as a circular cavity resonator, the far field electric and magnetic field components are obtained using the cavity model[2] and are given in the Appendix. Accordingly, the theoretical radiation patterns obtained using Matlab software for the E and H planes are shown in Fig. 4. The radiation patterns in both planes are very broad with a full-power-beam-width of  $180^\circ$  which can provide hemispherical coverage.

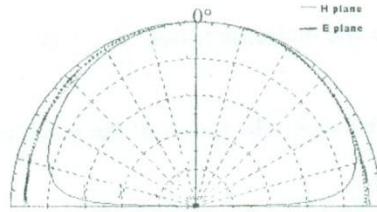


Fig. 4. Theoretical E and H plane radiation patterns of circular patch antenna

### Resonance frequency

The resonance frequency of the dominant resonant mode, the  $TM_{110}$  mode, is given by,

$$f_{r(110)} = 1.841 / (2 \pi a_e \sqrt{\mu_0 \epsilon_0 \epsilon_r}) \dots \dots \dots (1)$$

where  $a_e$  is the effective radius of the patch which has an actual radius “a” and it is given by,

$$a_e = a \left[ 1 + (2h / \pi a \epsilon_r) \left\{ (\ln (\pi a / 2h)) + 1.7726 \right\} \right]^{1/2} \dots \dots \dots (2)$$

The patch appears bigger than its geometrical size due to the effect of the fringing fields. For a resonance frequency of 1.6GHz, the value of effective radius  $a_e$  was obtained from equation (1). For this value of  $a_e$ , the required radius of the patch was obtained from equation (2) for a substrate of known thickness and  $\epsilon_r$ . The substrate used had an  $\epsilon_r$  of 2.91 and a thickness of 1.6mm. This gives a value of 31.31mm for the radius of the patch.



### Input impedance at resonance

In the cavity model, the patch is considered as a lossy resonator and the input conductance at resonance is calculated from the power radiated and the power dissipated. Accordingly, the input conductance is given by,

$$G_{in} = G_r + G_d + G_c \dots \dots \dots (3)$$

where  $G_r$  = conductance due to the radiation.

$G_d$  = conductance due to the surface wave losses in the dielectric.

$G_c$  = conductance due to the heat losses

It is shown that,

$$G_r = ((k_0 a_e)^2 / 480) \left[ \int_0^{\pi/2} (J_{02}^2 + \cos^2(\theta) J_{02}^2) \sin(\theta) d\theta \right] \dots \dots \dots (4)$$

where  $J_{02} = J_0 - J_2$  and  $J_{02} = J_0 + J_2$

Neglecting the surface wave and dielectric losses,  $G_{in} = G_r$

$$R_{in} = 1 / G_r \dots \dots \dots (5)$$

The input resistance  $R_{in}$  varies along the radius of the patch and it's value at any radius  $r_0$  is give by,

$$R_{in}(r = r_0) = (1 / G_r) \left[ J_m^2(kr_0) / J_m^2(ka_e) \right] \dots \dots \dots (6)$$

For the dominant  $TM_{110}$  mode, the variation of  $G_r$  with the effective radius obtained from equation (4), is shown graphically in Fig:5.

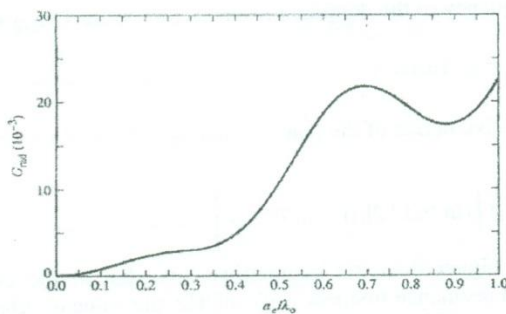


Fig:5 Variation of the radiation conductance at resonance as a function of the effective radius of the patch

The  $50\Omega$  inset feeding point to the patch was derived from the above conductance curve and equation(6).

### Circular polarization

The circular patch would normally radiate linearly polarized waves. Circular polarization can be obtained if two orthogonal modes of equal amplitude are excited with a  $90^\circ$  time-phase difference between them. This can be obtained using different feed arrangements. It can also be achieved by introducing perturbation segments to the basic patch shape or in other words, using mode de-tuning.

For the lowest order mode, which is the  $TM_{110}$  mode inside the patch, the usual method adopted is to use two feeds with proper angular separation. Using two coaxial feeds separated by a  $90^\circ$  angle, two fields that are orthogonal to each other are generated. To obtain a  $90^\circ$  time-phase difference, a  $90^\circ$  hybrid is used as shown in Fig. 6. This dual fed antenna gives a compact antenna with circular polarization but introduces additional losses.

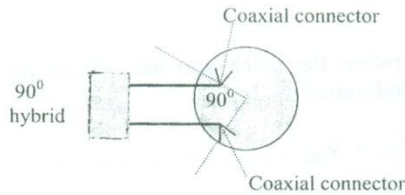


Fig. 6. Circular patch fed with coax and a  $90^\circ$  hybrid

Therefore to overcome the problem of unwanted additional losses, the mode de-tuning method was used in this design to obtain circularly polarized waves. This method has the added advantage that it requires only one feed point.

### Mode de-tuning method for circular polarization

The electric field inside the circular patch is given by equation (7).

$$E_z = E_0 J_1(kr) \cos(\phi) \dots\dots\dots(7)$$

To obtain circular polarization, two feed points with a  $90^\circ$  angular separation is selected to produce orthogonal fields. Hence equation (7) would become,

$$E_{z+\phi+90^\circ} = E_0 J_1(kr) \cos(\phi + 90^\circ) \dots\dots\dots(8)$$

In the mode de-tuning method  $E_{z+\phi+90^\circ}$  is virtually obtained with a single feed by adding perturbation segments, [1],[5] as shown in Fig. 7. This produces two orthogonal slightly de-tuned resonance modes, one mode with a phase lead of  $45^\circ$  and the other with phase lag of  $45^\circ$ . Thus this is a slightly de-tuned pair of orthogonal modes with a phase difference of  $90^\circ$ . Therefore the total field is due to the slightly de-tuned pair which is given by,



$$E_z = E_0 J_1(kr) \cos(\phi) + E_0 J_1(kr) \cos(\phi + 90^\circ) \dots (9)$$

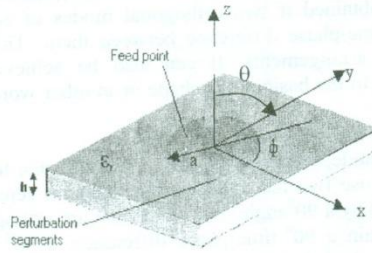


Fig:7 Circular patch with perturbation segments

The total voltage between the patch and the ground plane is the sum of the voltages due to each individual mode.

$$V_{in} = V_{m1} + V_{m2} \dots (10)$$

Therefore the network model of the circuit can be expressed as a combination of two parallel resonance circuits as shown in Fig. 8.

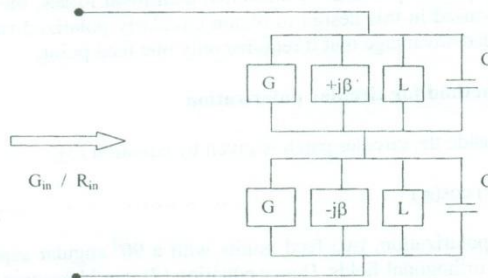


Fig. 8. Equivalent Circuit of the patch with two slightly detuned modes of the patch

$+j\beta$  and  $-j\beta$  are the susceptances of the de-tuned modes. At resonance the input impedance is real and it is equal to the reciprocal of conductance.

$$R_{in} = 1 / G_{in} \dots (11)$$

The value of the input resistance,  $R_{in}$  is necessary to obtain the correct inset point to feed the patch with the 50 ohm coaxial cable.

### DESIGN OF THE CIRCULARLY POLARIZED CIRCULAR PATCH ANTENNA

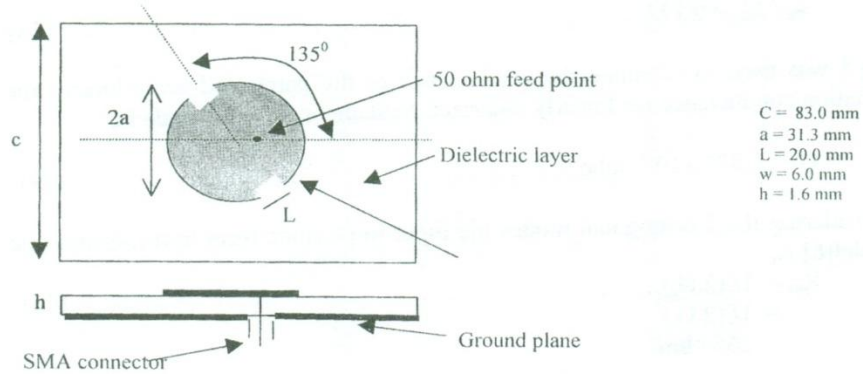


Fig. 9. Geometry of the patch for circularly polarised waves

#### Radius of the patch

In order to calculate the radius of the patch equations (1) and (2) can be rearranged as,

$$a = F / \{ 1 + (2h / F\pi\epsilon_r) (\ln(\pi F / 2h) + 1.7726) \}^{1/2} \dots\dots\dots(12)$$

$$\text{where } F = 8.791 \times 10^9 / f_r \sqrt{\epsilon_r} \dots\dots\dots(13)$$

Design frequency  $f_r = 1.6$  GHz,  $\epsilon_r = 2.91$ ,  $h = 1.6$  mm therefore the radius of the patch,

$$a = 31.31 \text{ mm} \dots\dots\dots(14)$$

#### Area of the perturbation segments

Area of the circular patch

$$S = 30.79 \text{ cm}^2 \dots\dots\dots(15)$$

The area of the perturbation segment  $\Delta S$  was selected to obtain an optimum axial ratio[3], as follows:-

$$\begin{aligned} \Delta S &= 0.04 S \dots\dots\dots(16) \\ &= 1.2 \text{ cm}^2 \end{aligned}$$

The dimensions of each perturbation segment are,

$$L = 20.0 \text{ mm}, w = 6.0 \text{ mm} \dots\dots\dots(17)$$



$$L = 20.0 \text{ mm}, w = 6.0 \text{ mm} \dots\dots\dots(17)$$

### Input impedance of the patch

In this design for a 1.6 GHz frequency of operation,

$$a_c / \lambda_0 = 0.172 \dots\dots\dots(18)$$

Fig.5 was used to calculate the conductance of the patch and accordingly the radiation conductance for linearly polarized fundamental  $TM_{110}$  mode is,

$$G_r = 1.875 \times 10^{-3} \text{ mho} \dots\dots\dots(19)$$

Considering the 2 orthogonal modes the input impedance from transmission line model[6] is,

$$\begin{aligned} R_{in} &= 1 / (2.G_r) \dots\dots\dots(20) \\ &= 1 / (2.G_r) \\ &= 266 \text{ ohm} \end{aligned}$$

A plot of equation (6) as given in Fig:10, was used to obtain a 50ohm inset feed point on the patch[7] so that the inner conductor of the SMA connector could be directly soldered to the selected feed point.

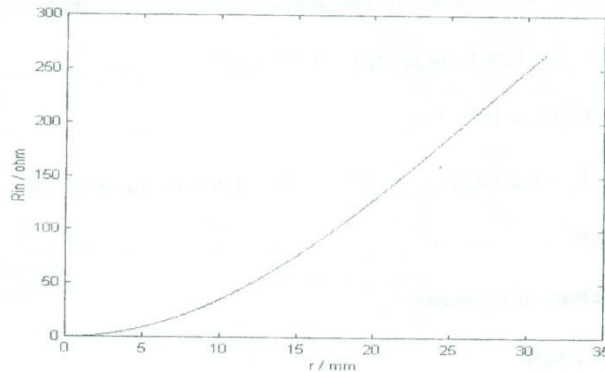


Fig. 10. Variation of the input impedance with radial distance

### OBSERVATIONS AND RESULTS

The far field radiation pattern measurements and gain measurements for the antenna were made using the experimental set up shown in Fig:11.

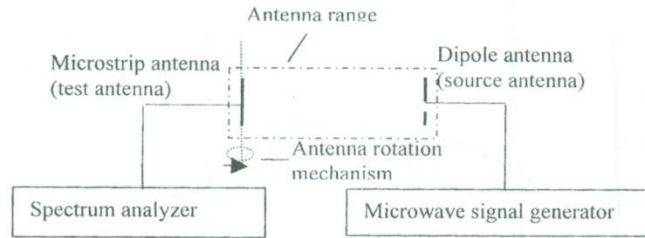


Fig. 11. Block diagram of typical instruments for antenna measurements

(a) With the test antenna as a receiving antenna the radiation patterns for the E and H planes were obtained by transmitting a signal of frequency 1.6 GHz, from a half-wave dipole antenna. The observations are given in Fig.12. The dipole antenna was kept vertical so that in the horizontal plane it produced an omnidirectional radiation pattern.

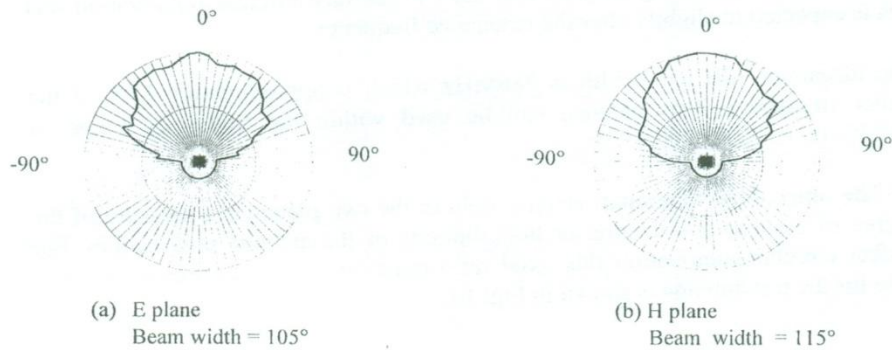


Fig: 12 Measured Radiation Patterns

The radiation pattern of the test antenna obtained experimentally shows a broad single lobe. It could provide nearly hemispherical coverage although the experimental radiation patterns are not as broad as the theoretical patterns. However they showed a large beam-width of nearly 110° in both planes. As mentioned before, a hemispherical radiation pattern for the vehicular antenna is an essential requirement for MSAT applications in order to communicate from any angle of elevation except near grazing. The circular patch antenna that was designed shows a satisfactory radiation pattern for the purpose of MSAT applications.

(b) The gain measurements were similarly taken using the same set up shown in Fig:11. Observations are given in Fig:13. The gain was estimated with respect to a half-wave dipole and the gain with respect to an isotropic antenna was estimated assuming that the gain of the dipole antenna is 2.15dBi. Antenna gain was measured for a set of frequencies in the range of 1.1 GHz to 1.7 GHz.

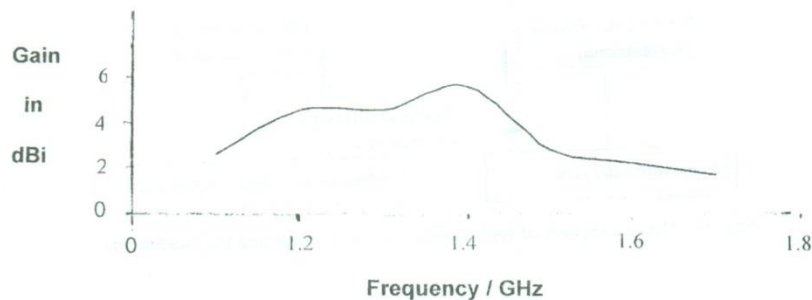


Fig. 13. Gain characteristics with frequency

The antenna was designed for a frequency of 1.6GHz. However the measured antenna gain is highest at 1.4GHz and it has a value of 5.71dBi. This is due to the fact that mode de-tuning method was used to produce circular polarization and this is expected to slightly alter the resonance frequency.

The measured 3dB bandwidth is 286MHz which is approximately 17% of the center frequency. This antenna can be used within the frequency range of 1.114GHz to 1.686GHz.

(c) The ratio of the maximum electric field in the two planes is a measure of the degree of circular polarization or the ellipticity of the antenna polarization. For perfect circular polarization this axial ratio must be unity. The measured axial ratio for the test antenna is shown in Fig: 14.

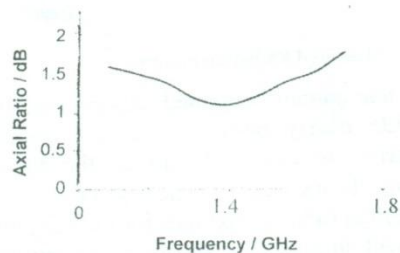


Fig. 14. Measured axial ratio of the test antenna

At 1.4GHz, the axial ratio is unity and polarization is perfectly circular. However, in the frequency range where the gain is high, the axial ratio varies between 1 and 1.5 and therefore the polarization is not exactly circular but elliptical. This however is acceptable for the MSAT application considered.

## CONCLUSIONS

The circular patch operating in the  $TM_{110}$  dominant mode was used to design a circular patch antenna for circular polarization. Cavity model approach was used to obtain the E and H plane radiation patterns, the resonance frequency, the input impedance and the input impedance variation with radius. MatLab software was used for the simulations. Mode de-tuning method was used to obtain circular polarization, with the addition of perturbation segments to the circular patch to obtain RHCP. A 50 ohm matched inset feed point was selected so that the patch could be directly fed using a SMA connector and a coaxial line. This eliminated the use of any microstrip transmission line which would have introduced additional losses and also caused space constraints. The circular patch was designed on epoxy glass fiber having a  $\epsilon_r$  of 2.91 which is commercially available. Measured E and H plane radiation patterns show nearly hemispherical radiation patterns in both planes and therefore the antenna appears promising for the purpose of communication for MSAT applications. Measured gain is 5.71dBi which is a reasonable value and has a band-width of approximately 17% of the center frequency. The band-width in terms of circular polarization is 280MHz about 1.4GHz. This antenna can be used in the frequency range 1.114 GHz to 1.686 GHz which is used for MSAT communications. Improvement of the gain should be possible with improvements of the in-house fabrication method used.

## Appendix: Fields within the cavity & Radiated Field

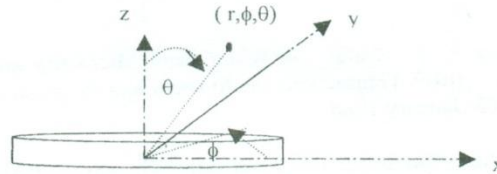


Fig. 15 Circular cavity

Fields within the cavity are given by equations (1) to (4).

$$E_z = E_0 J_1(kr) \cos(\phi) \dots (1)$$

$$H_\phi = j (E_0 / \omega \mu_0 r) J_1(kr) \sin(\phi) \dots (2)$$

$$H_z = j (E_0 / \omega \mu_0) J_1(kr) \cos(\phi) \dots (3)$$

$$E_\phi = E_\theta = H_r = 0 \dots (4)$$

The *far field* or the radiated field derived from the field within the cavity are given by equations (5) and (6).

$$E_\theta = -j \{ k_0 a_e V_0 e^{-jk_0 r} / 2r \} \{ \cos(\phi) J'_{02} \} \dots (5)$$

$$E_\phi = -j \{ k_0 a_e V_0 e^{-jk_0 r} / 2r \} \{ \cos(\theta) \sin(\phi) J_{02} \} \dots (6)$$

$$\text{where } J'_{02} = J_0(k_0 a_e V_0 \sin(\theta)) - J_2(k_0 a_e V_0 \sin(\theta)) \dots (7)$$



$$J_{02} = J_0 (k_0 a_e V_0 \sin(\theta)) + J_2 (k_0 a_e V_0 \sin(\theta)) \dots (8)$$

where  $a_e$  = effective radius of the patch

Therefore the fields in the principle planes, the E plane and the H plane can be obtained from the above equations.

For the E-plane,  $\phi = 0^\circ, 180^\circ, 0^\circ \leq \theta \leq 90^\circ$

$$E_\theta = -j \{k_0 a_e V_0 e^{-jk_0 r} / 2r\} \{J'_{02}\} \dots (9)$$

$$E_\phi = 0 \dots (10)$$

and for the H-plane,  $\phi = 90^\circ, 270^\circ, 0^\circ \leq \theta \leq 90^\circ$

$$E_\theta = 0 \dots (11)$$

$$E_\phi = j \{k_0 a_e V_0 e^{-jk_0 r} / 2r\} \{\cos(\theta) J_{02}\} \dots (12)$$

## REFERENCES

- [1] James J.R, "Microstrip Antenna Theory and design" IEE Electromagnetic wave series, 1986
- [2] Jan Sakora, " Spectrum Licence " <http://strategis.ic.gc.ca/SSI/sf/tmilicen.pdf>, 1999
- [3] Balanis C.A., "Antenna Theory and Design" Harper & Row, New York, 1992
- [4] Bhattacharyya A. K, Shafal, "A Wider band Microstrip antenna for Circular Polarization " ,IEEE Transactions on Antenna and Propagation, Vol FB-36, No 2, pp. 157-163 January 1988.
- [5] Hua-Ming Chen, "On the circular Polarization Operation of Annular-Ring Microstrip Antennas" , IEEE Transactions on Antenna and Propagation, Vol AU-47, No 8, pp. 1289-1292, August 1999.
- [6] Micheal H. Thursby, "Derivation of the Rectangular Microstrip Patch Antenna Radiation Pattern " , Florida Institute of Technology, ASL Technical Journal, Report No 7. [http://www.ee.fit.edu/electrical/asl\\_page/journal/report7/report~7.htm](http://www.ee.fit.edu/electrical/asl_page/journal/report7/report~7.htm), July 2001
- [7] Jui-Han Lu, Kai-Ping Yang, "A Simple Design for Single-feed Circularly-Polarized Microstrip Antennas", Department of Electronic Communication Engineering NKIMT Taiwan , Prac.Natl.Sei Counc. ROC(A) Vol. 24, No. 2, pp. 130-133, 2000
- [8] John H, "Seven-Element Circularly Polarized Patch Antenna", Glenn Research Center Ohio, <http://www.nasatech.com/Briefs/July99/LEW16713.html>, July 2001.